J|A|C|S ARTICLES

Published on Web 02/15/2010

Diverted Total Synthesis Leads to the Generation of Promising Cell-Migration Inhibitors for Treatment of Tumor Metastasis: *In vivo* and Mechanistic Studies on the Migrastatin Core Ether Analog

Thordur Oskarsson,[†] Pavel Nagorny,[‡] Isaac J. Krauss,[‡] Lucy Perez,[‡] Mihirbaran Mandal,[‡] Guangli Yang,[§] Ouathek Ouerfelli,[§] Danhua Xiao,[∥] Malcolm A. S. Moore,[∥] Joan Massagué,[†,⊥] and Samuel J. Danishefsky*[,‡,#]

Cancer Biology and Genetics Program, Cell Biology Program, Laboratory for Bioorganic Chemistry, Organic Synthesis Core Facility, Howard Hughes Medical Institute, Memorial Sloan-Kettering Cancer Center, 1275 York Avenue, New York, New York 10065, and Department of Chemistry, Columbia University, Havemeyer Hall, 3000 Broadway, New York, New York 10027

Received December 1, 2009; E-mail: s-danishefsky@ski.mskcc.org

Abstract: A significantly simpler analog of the natural product migrastatin, termed migrastatin ether (ME), has been prepared and evaluated. Both *in vivo* and *in vitro* studies indicate that ME exhibits a concentration-dependent inhibitory effect on migration of breast cancer cells.

Introduction

Despite extensive research directed to the prevention, detection, and treatment of various cancers, one of the important factors regarding the high mortality rate of various tumors is the phenomenon of tumor metastasis.[1] Much remains to be accomplished in finding new strategies for dealing with the immense problem of metastasis. Such efforts are well-justified, since success in this regard could play a major role in reducing the ravages of cancer. We describe the discovery of a promising cancer cell migration inhibitor, **2**, which could have significant potential for attenuating the progression of metastasis.

The starting point for this investigation was the reported isolation of a new polyketide natural product from *Streptomyces* sp. MK929-43F1 by Imoto and co-workers.[2] Shortly afterward, it was recognized that this product is a migration inhibitor of cancer cells with IC_{50} values in the micromolar range. Accordingly, the natural product was named migrastatin (**1**). This initial report prompted us, as well as others, to pursue the total synthesis of migrastatin.[3] In addition to the interesting chemistry level issues associated with such a goal, we were also motivated by the aim of preparing simplified and more potent cancer cell migration inhibitors using the logic of diverted total synthesis. Indeed, our group reported the inaugural total synthesis and the *in vitro* biological evaluation of **1** as well as several fully synthetic analogs (Figure 1).[4]

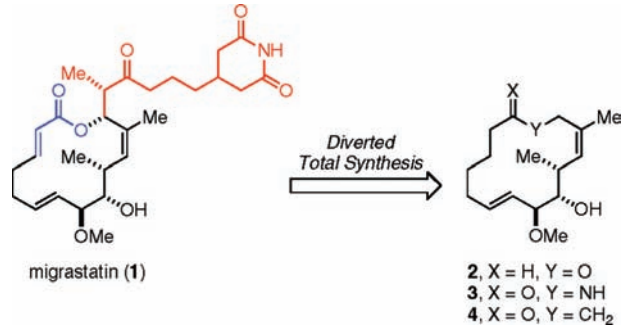

Figure 1. Migrastatin and synthetic analogs.

Remarkably, it was discovered in the context of those studies that *deletion of the entire glutarimide side chain, as well as the*

[†] Cancer Biology and Genetics Program, Memorial Sloan-Kettering Cancer Center.
[‡] Laboratory for Bioorganic Chemistry, Memorial Sloan-Kettering Cancer Center.
[§] Organic Synthesis Core Facility, Memorial Sloan-Kettering Cancer Center.
[∥] Cell Biology Program, Memorial Sloan-Kettering Cancer Center.
[⊥] Howard Hughes Medical Institute, Memorial Sloan-Kettering Cancer Center.
[#] Department of Chemistry, Columbia University.

(1) (a) Hedley, B. D.; Winquist, E.; Chambers, A. F. *Expert Opin. Ther. Targets* **2004**, *8*, 527–536. (b) Perez, L.; Danishefsky, S. J. *ACS Chem. Biol.* **2007**, *2*, 159–162.
(2) (a) Nakae, K.; Yoshimoto, Y.; Sawa, T.; Homma, Y.; Hamada, M.; Takeuchi, T.; Imoto, M. *J. Antibiot.* **2000**, *53*, 1130–1136. (b) Nakae, K.; Yoshimoto, Y.; Ueda, M.; Sawa, T.; Takahashi, Y.; Naganawa, H.; Takeuchi, T.; Imoto, M. *J. Antibiot.* **2000**, *53*, 1228–1230. (c) Takemoto, Y.; Nakae, K.; Kawatani, M.; Tahahashi, Y.; Naganawa, H.; Imoto, M. *J. Antibiot.* **2001**, *54*, 1104–1107. (d) Nakamura, H.; Takahashi, Y.; Naganawa, H.; Nakae, K.; Imoto, M.; Shiro, M.; Matsumura, K.; Watanabe, H.; Kitahara, T. *J. Antibiot.* **2002**, *55*, 442–444.
(3) (a) Gaul, C.; Danishefsky, S. J. *Tetrahedron Lett.* **2002**, *43*, 9039–9042. (b) Gaul, C.; Njardarson, J. T.; Danishefsky, S. J. *J. Am. Chem. Soc.* **2003**, *125*, 6042–6043. (c) Reymond, S.; Cossy, J. *Eur. J. Org. Chem.* **2006**, 4800–4804. (d) Reymond, S.; Cossy, J. *Tetrahedron* **2007**, *63*, 5918–5929.
(4) (a) Njardarson, J. T.; Gaul, C.; Shan, D.; Huang, X.-Y.; Danishefsky, S. J. *J. Am. Chem. Soc.* **2004**, *126*, 1038–1040. (b) Gaul, C.; Njardarson, J. T.; Shan, D.; Dorn, D. C.; Wu, K.-D.; Tong, W. P.; Huang, X.-Y.; Moore, M. A. S.; Danishefsky, S. J. *J. Am. Chem. Soc.* **2004**, *126*, 11326–11337. (c) Shan, D.; Chen, L.; Njardarson, J. T.; Gaul, C.; Ma, X.; Danishefsky, S. J.; Huang, X.-Y. *Proc. Natl. Acad. Sci. U.S.A.* **2005**, *102*, 3772–3776.

 10.1021/ja9101503

Scheme 1. Synthesis of Migrastatin Core Ether **2**[a]

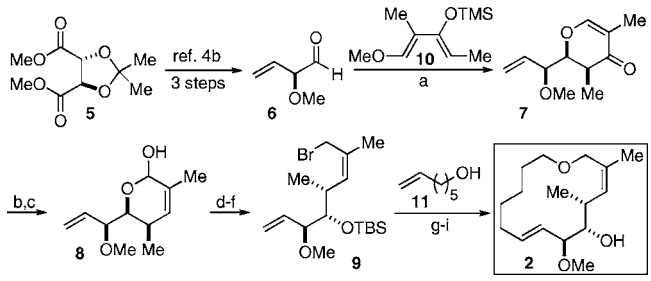

[a] Key: (a) (1) **10**, $TiCl_4$, DCM, −78 °C; (2) TFA, DCM; 87%; (b) $LiBH_4$, MeOH, THF, −10 °C; (c) CSA, H_2O, THF, reflux; (d) $LiBH_4$, MeOH, THF; 73%, three steps; (e) PPh_3, CBr_4, CH_3CN, 2,6-lutidine, rt, 85%; (f) TBSOTf, 2,6-lutidine, DCM, −15 °C, 91%; (g) **11**, NaH, THF, TBAI, 0 °C to rt; 90%; (h) Grubbs-II cat. 20%, toluene, reflux; 75%; (i) HF·Py, THF, 0 °C to rt, 90%.

α,*β-unsaturated lactone moieties, from the migrastatin-like structure did not abrogate inhibition of cell migration.* Indeed, the "des-side chain" compounds are in some cases strikingly (10^3) more potent than is **1**.[4] On the basis of this study, we selected several even more deeply simplified analogs of **1**: migrastatin core ether (**2**, ME), migrastatin core lactam (**3**), and migrastatin core ketone (**4**, MK) for further evaluation. Although both **3** and **4** have shown promising results in their ability to selectively inhibit cancer cell migration both *in vitro* and *in vivo*,[4] the simplicity of structure **2** makes it a particularly attractive candidate for potential development. In this study, we describe the total synthesis and *in vivo* biological evaluation of migrastatin analog **2**, as demonstrated in mouse models. As will be shown herein, compound **2** exhibits promising properties which could well be exploited for the suppression of metastasis.

In synthesizing analog **2**, we built upon the findings of our total synthesis of migrastatin itself (**1**).[3a,b] The assembly of **2** commenced from the known starting material **6**, prepared in three steps from commercially available 2,3-*O*-isopropylidene-1-tartrate **5** (Scheme 1).[3a,5] Chelation-controlled Lewis acid-catalyzed diene aldehyde cyclocondensation (LACDAC) of **6** with diene **10**[6] led to enone **7** in 87% yield as the single diastereomer.[7] With the three contiguous stereocenters thus established, the installation of the trisubstituted (Z)-alkene by a reduction/Ferrier rearrangement sequence was addressed. Thus, the reduction of **7**,[8] followed by treatment of the resultant allylic alcohol with aqueous CSA, provided lactol **8**,[9] which was reduced with $LiBH_4$, thereby providing the corresponding diol in 73% yield from **7**. The latter was converted to allylic bromide **9** by a two-step sequence (77% yield) involving selective bromination of the primary alcohol[10] followed by protection of the secondary alcohol as a *tert*-butyldimethylsilyl (TBS) ether. The reactive allylic bromide was etherified with compound **11** (90% yield),[11] and the resulting product was cyclized with the second-generation Grubbs catalyst.[12] Deprotection of the RCM product with HF·Py provided macrocycle **2** (68%, two steps).

Table 1. Inhibition of Transwell Cancer Cell Migration by Migrastatin Ether (ME, **2**) and Migrastatin Ketone (MK, **4**)[a]

		IC_{50} (μM)	
cell type	cell line	ME (**2**)	MK (**4**)
breast cancer (mouse)	4T1	0.47 ± 0.10	nd
breast cancer (human)	MDA-MB-231	0.30 ± 0.11	nd
breast cancer (human)	MDA-MB-435	0.37 ± 0.18	0.10
breast epithelium normal (human)	MCF10A	408 ± 80	nd

[a] Chemotaxis in response to a fetal calf serum gradient was measured after 12 h in 6 × 24 mm Transwell (Corning) with 8.0 μm pore size membrane inserts. Tumor cell migration was determined by counting cells attached to the underside of the membrane. ME or MK were added at 0 h to both upper and lower chambers over 5 log dilutions (1, 10, and 100 nM, 1 and 10 μM) with three wells at each dose. Data shown as half-maximal inhibitory concentration (IC_{50}) in micromol/L (μM); nd: not determined.

Results and Discussion

In the wake of this efficient synthesis of **2** came the opportunity to study its effect on biological processes. We first evaluated the effect of ME (**2**) on cell migration in the human breast cancer cell lines MDA-MB-231 (hereafter called MDA231) and MDA-MB-435, using an *in vitro* wound-healing assay. In one instance, we evaluated, *in vitro*, the relative potencies of ME (**2**) relative to that previously reported for MK (**4**).[13] ME (**2**) at 10 μM almost completely inhibited the migration of both cell lines induced by serum (data not shown). We then tested the compound in the Transwell cell-migration assay, where the compound inhibited 4T1 cells, MDA231, and MDA-MB-435 cell migration with IC_{50} in the range from 0.30 to 0.47 μM (Table 1). Interestingly, a ∼1000-fold higher concentration of ME (**2**) was required for comparable inhibition of normal human mammary epithelial MCF10A cells (IC_{50} = 408 μM). In contrast to the potent inhibitory effect on MDA231 cell migration, ME (**2**) did not have a comparable effect on cell proliferation, IC_{50} = 550 μM (data not shown). This suggests that the major biological effect of this compound (**2**) is inhibition of cell migration rather than inhibition of cell proliferation.

In the light of these results, we administered the compound (**2**) to the highly metastatic breast cancer cell line LM2-4175 (hereafter called LM2). LM2 cells are very aggressive and metastatic derivatives of MDA231 cells with increased propensity to form lung metastasis.[14] *In vitro* Transwell assays were done where LM2 cells were preincubated with incremental concentrations of ME (**2**) lasting 24 h before the assay. Migration of LM2 cells was significantly inhibited at concentrations of 2.5 and 5 μM (Figure 2). Furthermore, comparison of inhibitory effects of the core ether analog ME (**2**) and migrastatin (**1**) showed that ME exhibited a superior inhibitory effect at 5 μM concentration (Figure 3). Neither ME (**2**) nor migrastatin

(5) Lee, W. W.; Chang, S. *Tetrahedron: Asymmetry* **1999**, *10*, 4473–4475.
(6) Danishefsky, S. J.; Yan, C. F.; Singh, R. K.; Gammill, R. B.; McCurry, P. M., Jr.; Fritsch, N.; Clardy, J. *J. Am. Chem. Soc.* **1979**, *101*, 7001–7008.
(7) (a) Danishefsky, S. J. *Aldrichimica Acta* **1986**, *19*, 59–68. (b) Danishefsky, S. J. *Chemtracts* **1989**, *2*, 273–289. (c) Danishefsky, S. J.; Pearson, W. H.; Harvey, D. F.; Maring, C. J.; Springers, J. P. *J. Am. Chem. Soc.* **1985**, *107*, 1256–1268.
(8) Luche, J. L.; Gemal, A. L. *J. Am. Chem. Soc.* **1979**, *101*, 5848–5849.
(9) Ferrier, R. J. *J. Chem. Soc.* **1964**, 5443–5449.
(10) Appel, R. *Angew. Chem., Int. Ed. Engl.* **1975**, *14*, 801–811.
(11) Inanaga, J.; Hirata, K.; Saeki, H.; Katsuki, T.; Yamaguchi, M. *Bull. Chem. Soc. Jpn.* **1979**, *52*, 1989–1993.
(12) Scholl, M.; Ding, S.; Lee, C. W.; Grubbs, R. H. *Org. Lett.* **1999**, *1*, 953–956.
(13) The relative merits of compounds **2** and **4** as candidates for further development en route to the clinic are being evaluated. Toward that end, it will be necessary to conduct the extensive studies described herein on MK (**4**).
(14) Minn, A. J.; Gupta, G. P.; Siegel, P. M.; Bos, P. D.; Shu, W.; Giri, D. D.; Viale, A.; Olshen, A. B.; Gerald, W. L.; Massagué, J. *Nature* **2005**, *436*, 518–524.
(15) Minn, A. J.; Kang, Y.; Serganova, I.; Gupta, G. P.; Giri, D. D.; Doubrovin, M.; Ponomarev, V.; Gerald, W. L.; Blasberg, R.; Massagué, J. *J. Clin. Invest.* **2005**, *5*, 44–55.

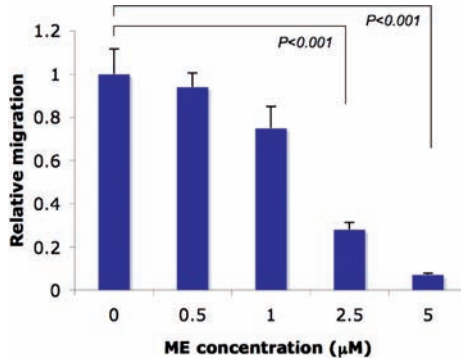

Figure 2. ME-mediated inhibition of LM2 cell migration. Transwell migration assay where LM2 cells were pretreated for 24 h with compound **2** (ME) at the indicated concentrations. *P*-values were determined using two-tailed Student's *t* test.

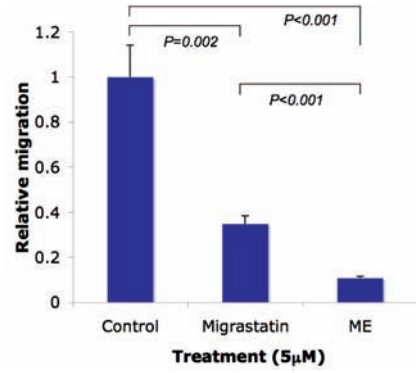

Figure 3. Comparison of ME (**2**) and migrastatin (**1**) inhibitory activity. LM2 cells were pretreated with 5 μM ME or migrastatin, and the migration ability was assessed with a Transwell assay. *P*-values were obtained using two-tailed Student's *t* test.

(**1**) affected the viability of LM2 cells at these concentrations (Tables 1 and 2 of the Supporting Information).

ME (2) Treatment in a Human Breast Cancer Xenograft Model Inhibited Tumor Invasion and Metastasis and Prolonged Overall Survival in NOD/SCID Mice. To assess the ability of ME (**2**) to inhibit tumor metastasis *in vivo*, we utilized luciferase-based noninvasive whole animal bioluminescent imaging in a xenograft breast cancer model in NOD/SCID mice transplanted with MDA231 cells stably expressing the HSV-TK-eGFP-luciferase (TGL) reporter protein.[15] Mice were inoculated with 1×10^7 tumor cells in the abdominal mammary gland area, and groups of five mice were given ME (**2**) (40 mg/kg) ip three times per week beginning either at day 1, when the tumor cells were injected (ME (**2**)-pregroup), or from day 15, when the primary tumors were surgically resected (ME (**2**)-postgroup). The control mice were treated with PBS. Tumor volume and distribution were measured by serial bioluminescent imaging (see Figure 3 of the Supporting Information). At the time of surgical resection, 50% of control mice had metastases and 85% had tumors that invaded into the muscle layer and peritoneal membrane. ME (**2**)-pretreatment markedly localized the tumor to the original injection site. One week after resection, imaging showed extensive metastases in control mice, a 47% reduction in metastases in the ME (**2**)-postgroup, and a significant 87% reduction in the ME (**2**)-pregroup (Figure 4A). ME (**2**)-post-treatment had little effect on overall survival, with mortality attributed to tumor growth at sites of metastasis established prior to ME (**2**) treatment and to recurrence of tumor at the resection site (Figure 5). The ME (**2**)-pregroup showed significantly prolonged overall survival with mortality attributed to recurrence of tumor growth at the site of resection rather than in metastatic sites (Figure 5). This was confirmed by histopathological studies at 2 weeks postresection showing in the control group a systemic carcinomatosis involving almost all visceral organs and tissues including liver, lung, spleen, pancreas, mesenteric lymph nodes, kidney, and multifocal bone marrow sites (data not shown). ME (**2**)-post-treatment did not prevent systemic carcinomatosis, with the exception of bone marrow that, in contrast to the control mice, was not a site of metastasis. In marked contrast, in the ME (**2**)-pregroup, carcinoma was confined to the tumor resection site in the mammary fat pad and there was no evidence of systemic carcinomatosis. There was no significant body-weight loss in the treatment groups compared with the control, indicating that at this dosage ME (**2**) was not toxic to the animals (data not shown).

In another study comparing two dose levels of ME **(2)**, NOD/SCID mice were again injected in the abdominal mammary fat pad with 1×10^7 MDA231 cells. At day 1, groups of eight mice were injected with low dose ME (**2**) (40 mg/kg ip 3× weekly), high dose ME (**2**) (200 mg/kg ip 3× weekly), or control PBS. After 4 weeks the primary tumors were surgically resected and bioimaging for metastasis tumor was undertaken weekly. One week after resection, imaging showed extensive metastases in control mice with a significant 88−93% reduction in

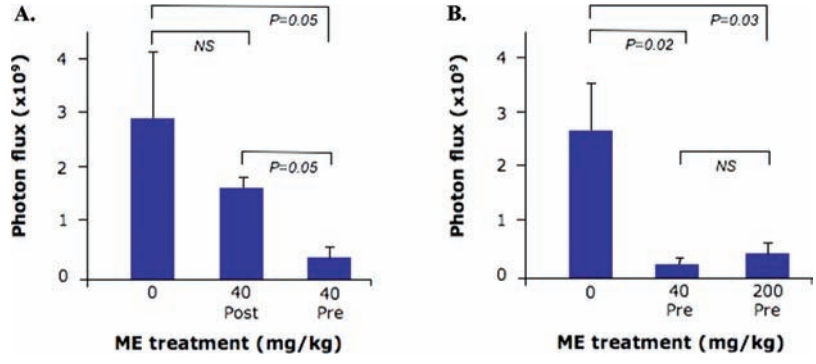

Figure 4. ME (**2**) inhibition of metastasis in mice inoculated with MDA231 cells as determined by bioimaging at 1 week after resection of primary tumor. MDA231 cells were injected into the mammary fat pad of NOD/SCID mice. The mice were treated with indicated dosages of ME (**2**), three times per week. (A) ME (**2**) treatment (40 mg/kg) begun at day 1 (Pre) or day 15 (Post) after tumor inoculation. Primary tumor was resected at 2 weeks and tumor metastasis determined by bioimaging at 3 weeks. (B) ME (**2**) treatment (40 or 200 mg/kg) begun at day 1 after tumor inoculation. Primary tumor was resected at 3 weeks and tumor metastasis determined by bioimaging at 4 weeks. *P*-values were obtained using two-tailed Student's *t* test.

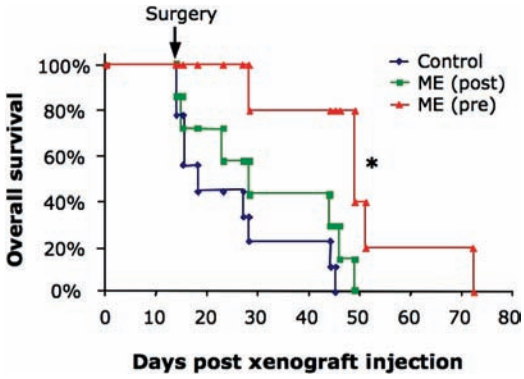

Figure 5. Kaplan−Meier survival curves of MDA231 tumor-bearing mice treated with high or low doses of ME (**2**) or PBS begun at the time of tumor transplantation. NOD/SCID mice injected with MDA231 cells and treated three times per week with 40 mg/kg ME (**2**) begun at the time of tumor engraftment (ME pre) or following resection of primary tumor at 2 weeks postengraftment (ME post). *$P = 0.005$. *P*-value was obtained using log-rank test.

metastases with both high and low dose ME (**2**) (Figure 4B). At 7 weeks, groups of mice were sacrificed and the lungs, liver, spleen, and thymus were surgically removed and imaged. There was extensive detectable metastatic growth of tumor in lungs and liver of control mice but none in the ME (**2**)-treated mice (Figure 1 of the Supporting Information). By 9 weeks there was detectable metastatic tumor in lungs and liver in the 40 mg/kg ME (**2**) group, but the 200 mg/kg high dose group had no detectable metastases at this time (Figure 1 of the Supporting Information). Within 50 days, all mice in the untreated control cohort had died. However, at this time point the survival within the ME-treated cohorts was 30% for 40 mg/kg and 50% for 200 mg/kg treatment (Figure 2 of the Supporting Information).

In a separate cohort of experiments, the ability of migrastatin core ether (**2**) to prevent lung metastasis of LM2 cells was studied. As mentioned, LM2 cells are originally derived from the MDA231 cells and have increased metastatic efficiency of seeding in lungs.[14] Taking advantage of an *in vivo* model with increased specificity, we set out to test the efficacy of ME as an inhibitor of metastasis by established mammary tumors. To assay metastatic activity *in vivo*, LM2 cells were inoculated orthotopically in the mammary fat pad of immunodeficient NOD/SCID mice. Mammary tumors were monitored and allowed to grow for 27 days before initiation of treatment (Figure 6). Animals were treated three times per week with **2** (ME) at 100 or 200 mg/kg dosage, and lung metastasis was determined by ex vivo bioluminescence imaging at day 42. The average luminescence was reduced by 2.5-fold with 100 mg/kg treatment of **2** and 4.5-fold with 200 mg/kg treatment of **2** (Figure 6B), indicating significant reduction in lung metastatic burden. Despite relatively high variability within cohorts, suppression of lung metastasis was statistically significant ($P < 0.05$) in cohorts treated with 200 mg/kg. Interestingly, on the basis of regular measurements of the mammary fat pad tumors, treatment with **2** did not significantly attenuate mammary tumor growth (Figure 6A), suggesting a selective effect on metastasis from established mammary tumors.

In order to assess the ability of **2** to inhibit the metastatic spread of cells that are already in circulation, a lung colonization assay based on inoculation of LM2 cells into the mouse venous system was performed. The treatment of the mice with **2** qualitatively exhibited a trend toward inhibition of metastatic outgrowth (Figure 2 of the Supporting Information). Five out

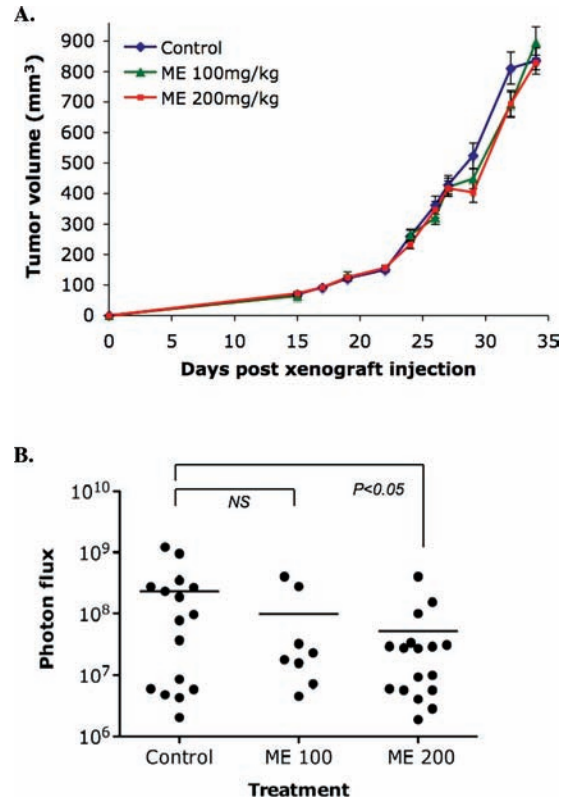

Figure 6. Analysis of mammary tumor growth and lung metastasis. (A) Mammary tumor growth. Luciferase transduced LM2 cells were injected bilaterally into the fourth mammary gland fat pad of NOD/SCID mice. The size of the mammary tumor was measured regularly using a caliper. Day 27 after injection, mice underwent treatment with ME 100 mg/kg, ME 200 mg/kg, or vehicle as control. The treatment was administered three times per week via intraperitoneal injection. Control, $n = 16$; ME 100 mg/kg, $n = 8$; ME 200 mg/kg, $n = 17$. (B) Lung metastasis at end point measured by luminescence. At day 42, mice were analyzed for lung metastasis by ex vivo bioluminescence, quantifying luciferase activity in the lungs. NS, not statistically significant; ME 100, ME 100 mg/kg; ME 200, ME 200 mg/kg. *P*-values were determined using two-tailed Student's *t* test.

of seven mice responded well, but due to high variability within the cohort, the effect did not achieve statistical significance. Together these results suggest that **2** can inhibit the migration of breast cancer cells *in vitro* and the dissemination of metastatic tumors *in vivo*.

Conclusion

In summary, a much simplified analog of migrastatin, termed migrastatin ether (**2**), has been prepared and evaluated. Both *in vivo* and *in vitro* studies indicate that **2** exhibits a concentration-dependent inhibitory effect on migration of MDA231 and LM2 breast cancer cells. Treatment with **2** did not reduce the viability of either MDA231 or LM2 cells in culture, nor did such treatment suppress the rate of growth of MDA231 or LM2 cells as mammary tumors. However, treatment with ME (**2**) appeared to increase survival of mice injected with MDA231 breast cancer cells. Also, treatment with ME (**2**), initiated at the time of engraftment, profoundly suppressed metastasis at 7 weeks, and at the highest dose used (200 mg/kg), there were no detectable metastases at 9 weeks (Figure 1 of the Supporting Information). Delaying administration of ME (**2**) for 2 weeks after tumor engraftment did not prolong survival, presumably because metastasis to multiple sites had already occurred and ME did not suppress metastatic tumor development once metastatic

tumor cells had seeded to multiple organs. These findings establish a specific effect on cellular migratory capabilities. Even at the highest doses used, ME was well-tolerated, suggesting that it could be used in settings requiring chronic administration. The tumor line used was from a patient with a metastatic tumor and it was thus not surprising that the xenografted tumor was releasing metastatic cells within the first two weeks of engraftment.

The data suggest possible clinical applications, for example, efficient resection of breast cancer at an early stage, followed by chronic ME (**2**) treatment. A combination of ME (**2**) with drugs that suppress tumor growth at the primary or metastatic sites should also be evaluated, and in this context, we have shown third-generation microtubule stabilizing epothilones such as fludelone and isofludelone to be highly effective against taxol-resistant breast tumors in xenograft models.[16]

Our findings establish a specific effect of ME (**2**) on tumor cellular migratory capabilities. Recently, we identified a set of 18 genes, whose expression in MDA231 and LM2 cells mediates lung metastatic activity.[14] This lung metastasis signature (LMS) is associated with lung relapse in breast cancer patients.[14] Most LMS genes encode secretory or cell surface proteins with the exception of fascin-1, which is an actin-bundling protein implicated in cancer cell migration.[17] A key role for fascin-1 in MDA231 cell migration and tissue infiltration has recently been demonstrated.[18] This evidence suggests that in MDA231 and LM2 cells ME interferes with a fascin-1-dependent migratory behavior. Although there is still need for optimization at the level of formulation and potency,[19] migrastatin macroether **2** already shows considerable promise as a specific inhibitor of cellular migration and has great potential for inhibiting metastatic dissemination.

We note in passing that the progression which led from migrastatin to compound **2** is very much in keeping with the discovery platform which we have termed diverted total synthesis (DTS).[20] In this modality, the achievements of total synthesis are channeled to provide access to otherwise inaccessible structural space built around high-pedigree structures such as small molecule natural products (SMNPs). Several other examples of the value of DTS for facilitating the discovery of very promising leads have been reported.[21]

Acknowledgment. This work was supported by NIH grants CA103823 (S.J.D.), CA126518 (J.M.), and CA129243 (J.M.); by the Alan and Sandra Gerry Metastasis Research Initiative (J.M.); and by a Cancer Research Institute Gar Reichman Award (M.M.). J.M. is an Investigator of the Howard Hughes Medical Institute. P.N. thanks the National Institutes of Health for a Ruth L. Kirschstein postdoctoral fellowship (CA125934-02). We thank Dr. George Sukenick, Hui Fang, and Sylvi Rusli of SKI's NMR core facility for mass spectral and NMR analysis and Rebecca Wilson for editorial assistance.

Supporting Information Available: Experimental procedures, copies of spectral data, and characterization (PDF). This material is available free of charge via the Internet at http://pubs.acs.org.

JA9101503

(16) Chou, T. C.; Zhang, X.; Zhong, Z. Y.; Li, Y.; Feng, L.; Eng, S.; Myles, D. R.; Johnson, R. Jr.; Wu, N.; Yin, Y. I.; Wilson, R. M.; Danishefsky, S. J. *Proc. Natl. Acad. Sci. U.S.A.* **2008**, *105*, 13157–13162.
(17) Hashimoto, Y.; Skacel, M.; Adams, J. C. *Int. J. Biochem. Cell Biol.* **2005**, *37*, 1787–1804.
(18) Kim, M. Y.; Oskarsson, T.; Acharyya, S.; Nguyen, D. X.; Zhang, X. H.; Norton, L.; Massagué, J. *Cell* **2009**, *139*, 1315–1326.
(19) Hennenfent, K. L.; Govindan, R. *Ann. Oncol.* **2006**, *17*, 735–749.
(20) Wilson, R.; Danishefsky, S. J. *J. Org. Chem.* **2006**, *71*, 8329–8351.
(21) (a) Rivkin, A.; Chou, T.-C.; Danishefsky, S. J. *Angew. Chem., Int. Ed.* **2005**, *44*, 2838–2850. (b) Yun, H.; Chou, T.-Ch.; Dong, H.; Tian, Y.; Li, Y.; Danishefsky, S. J. *J. Org. Chem.* **2005**, *70*, 10375–10380. (c) Wright, B. J. D.; Hartung, J.; Peng, F.; Van de Water, R.; Liu, H.; Tan, Q.-H.; Chou, T.-C.; Danishefsky, S. J. *J. Am. Chem. Soc.* **2008**, *130*, 16786–16790.